

Topological corner states in graphene by bulk and edge engineeringJunjie Zeng ^{1,2,*}, Chen Chen ^{3,*}, Yafei Ren,⁴ Zheng Liu,¹ Wei Ren,^{3,†} and Zhenhua Qiao ^{1,5,‡}¹CAS Key Laboratory of Strongly-Coupled Quantum Matter Physics, and Department of Physics, University of Science and Technology of China, Hefei, Anhui 230026, China²Chongqing Key Laboratory for Strongly Coupled Physics and Institute for Structure and Function, Department of Physics, Chongqing University, Chongqing 401331, China³International Center for Quantum and Molecular Structures, Materials Genome Institute, Physics Department, and Shanghai Key Laboratory of High Temperature Superconductors, Shanghai University, Shanghai 200444, China⁴Department of Materials Science and Engineering, University of Washington, Seattle, Washington 98195, USA⁵ICQD, Hefei National Laboratory for Physical Sciences at Microscale, University of Science and Technology of China, Hefei, Anhui 230026, China

(Received 18 February 2022; accepted 31 October 2022; published 23 November 2022)

Two-dimensional higher-order topology is usually studied in (nearly) particle-hole symmetric models, so that an edge gap can be opened within the bulk one. But more often the edge anticrossing deviates even into the bulk, where corner states are difficult to pinpoint. We address this problem in a graphene-based \mathbb{Z}_2 topological insulator with spin-orbit coupling and in-plane magnetization both originating from substrates through a Slater-Koster multiorbital model. The gapless helical edge modes cross inside the bulk, where the magnetization-induced edge gap is also located. After demonstrating its second-order nontriviality in bulk topology by a series of evidence, we show that a difference in bulk-edge on-site energy can adiabatically tune the position of the crossing/anticrossing of the edge modes to be inside the bulk gap. This can help unambiguously identify two pairs of topological corner states with nonvanishing energy degeneracy for a rhombic flake. We further find that the obtuse-angle pair is more stable than the acute-angle one.

DOI: [10.1103/PhysRevB.106.L201407](https://doi.org/10.1103/PhysRevB.106.L201407)

Introduction. It has been well established so far that topologically nontrivial phases in crystalline solid materials can be understood in a unified and consolidated mathematical picture in terms of a fiber bundle, constructed from Bloch wave functions over the first Brillouin zone as its base space, bearing a geometrical structure that is not globally direct-product decomposable (also referred to as with a global twisting of some kind) [1–5]. Typical examples are the quantum anomalous Hall effect [6–8] and quantum spin Hall effect [9–11], whose corresponding Bloch bundles are respectively categorized by the Chern class [12,13] and \mathbb{Z}_2 class [14–16], contributing therefore to their appellations as a Chern insulator and \mathbb{Z}_2 topological insulator. On the other hand, another relevant and intensively reiterated concept is “bulk-boundary correspondence,” not only because of its concreteness to comprehend, but also its prediction of perfect conducting channels with the potential for exploitation. Though efforts have been devoted to its formulation [17–25], in contrast, it still can hardly be considered beyond conjecture with respect to the whole research field of topological physics. One of its statements may read as follows: A system accommodating a nontrivial bulk phase has its gapless representatives on its one-less-dimension boundaries if it changes to a finite geometry. It

works, for example, for the aforementioned Chern insulator and \mathbb{Z}_2 topological insulator with a manifestation as gapless chiral and helical edge states, respectively. However, this relationship has to be modified at least for two cases: non-Hermitian [26–30] and higher-order topological systems [31–36]. In the former case, one-by-one situations need corresponding generalizations, and in the latter case there are simply no gapless boundary states at all on boundaries with unit-lower dimensions. Among various attempts, following several approved strategies [37–39], to rebuild it in a broader sense, as a consequence, e.g., one has to find smoking gun evidence as one-dimensional hinge states [40–42] and zero-dimensional corner states [39,43–46], respectively, in three- and two-dimensional topological systems. But these processes are not always easy to accomplish and one of the difficulties is represented by that in two-dimensional systems, the first-order gapless dispersion crosses outside of the bulk gap, making the “corner states within a gap within a gap” strategy no longer applicable.

In this Letter, we resolve this problem by using monolayer graphene as a prototypical system, which is widely adopted as an ideal arena for various topologically nontrivial phases [8,9,39,47–55]. Inspired by the *ab initio* research on a monolayer graphene system with bismuth ferrite as the substrate [56,57] (also see Sec. SI in the Supplemental Material [58]) and the higher-order topology generating routine by opening gaps for gapless boundary modes [39,59], we first confirm its bulk nontrivial topology despite a vanishing Chern number by

*These authors contributed equally to this work.

†Corresponding author: renwei@shu.edu.cn

‡Corresponding author: qiao@ustc.edu.cn

both the gapless evolution of the bulk Wannier charge center and the nonvanishing mirror-graded Zak phases ($\gamma_{\pm} = \pi$), and then we find (i) the tunability of the edge states by an adiabatic on-site energy difference between the bulk and the edge atoms, and (ii) an extra acute-angle pair of corner states degenerated on a different nonvanishing energy from that of the obtuse-angle pair. Those observations indicate that topological corner modes, as important evidence of higher-order nontrivial topology, may not be identifiable as directly as the topological gapless edge ones, and therefore might facilitate a step forward in deepening our understanding in the guiding rule of bulk-boundary correspondence. Additionally, because of the similarity in mathematical descriptive formalism [60–67], the issue raised and the solution provided for electronics here are also highly relevant for seeking localized states of a higher-order topological nature in phononic and photonic crystals [31,68–71], if the same strategy is followed.

System model. We employ the Slater-Koster multiorbital tight-binding model to describe the monolayer graphene in a 16-dimensional Hilbert space, $\mathcal{S} = \mathcal{S}_{\text{sublatt.}} \otimes \mathcal{S}_{\text{orbit.}} \otimes \mathcal{S}_{\text{spin.}}$, where the sublattice, atomic orbital, and spin subspaces $\mathcal{S}_{\text{sublatt./orbit./spin}}$ are spanned by the bases $\mathcal{B}_{\text{sublatt.}} = \{|A\rangle, |B\rangle\}$, $\mathcal{B}_{\text{orbit.}} = \{|s\rangle, |p_x\rangle, |p_y\rangle, |p_z\rangle\}$, and $\mathcal{B}_{\text{spin.}} = \{|\uparrow\rangle, |\downarrow\rangle\}$, respectively. By including the first-nearest-neighbor hoppings, the Hamiltonian reads

$$H = H_{\text{SK}} + H_{\text{SOC}} + H_{\text{M}} + H_{\text{AB}},$$

where H_{SK} , H_{SOC} , H_{M} , and H_{AB} are terms resulting from the wave function overlapping from the Slater-Koster method [72–75], atomic spin-orbit coupling (SOC), exchange field, and sublattice potential, respectively. These terms can be expressed in second-quantization form,

$$H_{\text{SK}} = \sum_{i\alpha} c_{i\alpha}^{\dagger} (\epsilon_{i\alpha} s_0) c_{i\alpha} + \sum_{(ij)\alpha\beta} c_{i\alpha}^{\dagger} (t_{\alpha\beta} s_0) c_{j\beta}, \quad (1)$$

$$H_{\text{SOC}} = \xi_{\text{SOC}} \sum_{i,\alpha\beta} c_{i\alpha}^{\dagger} (\mathbf{s} \cdot \mathbf{I})_{\alpha\beta} c_{i\beta}, \quad (2)$$

$$H_{\text{M}} = M \sum_{i\alpha} c_{i\alpha}^{\dagger} (\mathbf{s} \cdot \hat{\mathbf{n}}_{\text{M}}) c_{i\alpha}, \quad (3)$$

$$H_{\text{AB}} = U \sum_{i \in A, j \in B, \alpha} (c_{i\alpha}^{\dagger} c_{i\alpha} - c_{j\alpha}^{\dagger} c_{j\alpha}), \quad (4)$$

where i and j label the atomic position in real space and $\langle \dots \rangle$ means to sum over nearest neighbors. α and β take integer values from 0 to 3 and correspondingly stand for all four outer-shell atomic orbitals in $\mathcal{B}_{\text{orbit.}}$. The creation operator $c_{i\alpha}^{\dagger} = (c_{i\alpha\uparrow}^{\dagger}, c_{i\alpha\downarrow}^{\dagger})$ is understood with spin as its internal degree of freedom. The spin Pauli matrices are denoted as $\mathbf{s} = (s_x, s_y, s_z)$. Hereinbelow, all energies are measured in eV and the length is in the unit of lattice constant a , if not otherwise explicitly indicated.

Further details of Eq. (1) can be found in Sec. SII in the Supplemental Material [58]. In Eq. (2) the matrix element of the atomic spin-orbit coupling takes the form of the atomic-orbital subspace $\mathcal{B}_{\text{orbit.}}$ as [76,77]

$$(\mathbf{s} \cdot \mathbf{I}) = i \begin{pmatrix} 0 & 0 & 0 & 0 \\ 0 & 0 & -gs_z & s_y \\ 0 & gs_z & 0 & -s_x \\ 0 & -s_y & s_x & 0 \end{pmatrix}, \quad (5)$$

where $g = 1$ if not otherwise indicated. The parameter ξ_{SOC} is the atomic spin-orbit coupling strength and it is related to the “intrinsic spin-orbit coupling” strength as $t_2 = |\epsilon_s| \xi_{\text{SOC}}^2 / (18V_{sp\sigma}^2)$, where ϵ_s is the on-site energy of the s orbital relative to that of the p orbital [78]. The latter considers a second-nearest-neighboring hopping among p_z orbitals and is responsible for a bulk gap $\Delta E_{\text{bulk}} = 6\sqrt{3}t_2$ [9], which can be used as an estimation of the bulk gap in this Letter. The general form of magnetization term Eq. (3) has a unit vector $\hat{\mathbf{n}}_{\text{M}} = (\sin \theta_{\text{M}} \cos \phi_{\text{M}}, \sin \theta_{\text{M}} \sin \phi_{\text{M}}, \cos \theta_{\text{M}})$ specifying an arbitrary direction of the magnetization. In our consideration, we choose $\theta_{\text{M}} = \pi/2$ and $\phi_{\text{M}} = 0$, i.e., $\mathbf{M} = M\hat{\mathbf{e}}_x$, as it can be shown in the phase diagram in Fig. 1(c) that the in-plane direction of magnetization does not display its importance, concerning topological states.

Band structure and bulk topology. Before we start to search for corner states, it is highly necessary to confirm the nontrivial topology of the bulk system. With an in-plane magnetization, the system can host two phases, as depicted in Fig. 1. When the sublattice potential is larger ($|U| > |M|$), a quantum valley Hall phase appears [Fig. 1(a1)] with valley Chern numbers [8,79,80] $(C_K, C_{K'}) = (-1, 1)$ contributed by the Berry curvature in proximity of the two valleys [Figs. 1(a2) and 1(a3)]; whereas if $|U| < |M|$, a VW-shaped band structure takes form around the global band gap and the Brillouin zone corners [Fig. 1(b1)], however, the corresponding Chern number vanishes. In both cases, the in-plane direction of the magnetization is irrelevant, which can be drawn from Fig. 1(c), where one can see an isotropic phase border, namely the white dashed circle.

However, the latter state does not have to be trivial just because of a vanishing Chern number. Without explicit indication, we set a zero sublattice potential case hereafter. Then we can check the bulk topology with two methods: One is the bulk Wannier charge center (WCC) [81,82] (see Sec. SIII in the Supplemental Material [58]) and the other is the mirror-graded Zak phase. The former method generates the Wannier charge center evolution for the above quantum valley Hall effect and the other globally gapped state with a dominant in-plane magnetization in Figs. 2(a) and 2(b), respectively. The major difference is that the latter is gapless but the former is not, and the gapless Wannier charge center behavior indicates the nontrivial bulk topology.

Furthermore, a mirror operator in the working representation $(\mathcal{S}, \mathcal{B})$ can be found to have this form [83,84],

$$\mathcal{M}_x = \sigma_x \otimes \text{diag}\{1, -1, 1, 1\} \otimes (is_x), \quad (6)$$

whose determination is detailed in Sec. SIV of the Supplemental Material [58], to commute with the bulk Hamiltonian with a vanishing lattice momentum in the x direction (connecting two nearest carbon atoms): $[\mathcal{M}_x, H(0, k_y)] = 0$. The unitary operation \mathcal{U} that diagonalizes \mathcal{M}_x facilitates to direct-sum decompose $H(0, k_y)$ as

$$\mathcal{U}H(0, k_y)\mathcal{U}^{\dagger} = H_+(k_y) \oplus H_-(k_y). \quad (7)$$

Both $H_{\pm}(k_y)$'s spectra are globally gapped as shown in Figs. 2(c)–2(e), and they do not have much difference. Actually, every band is at least locally gapped from any other one. But neither of $H_{\pm}(k_y)$ owns a chiral symmetry, hence the

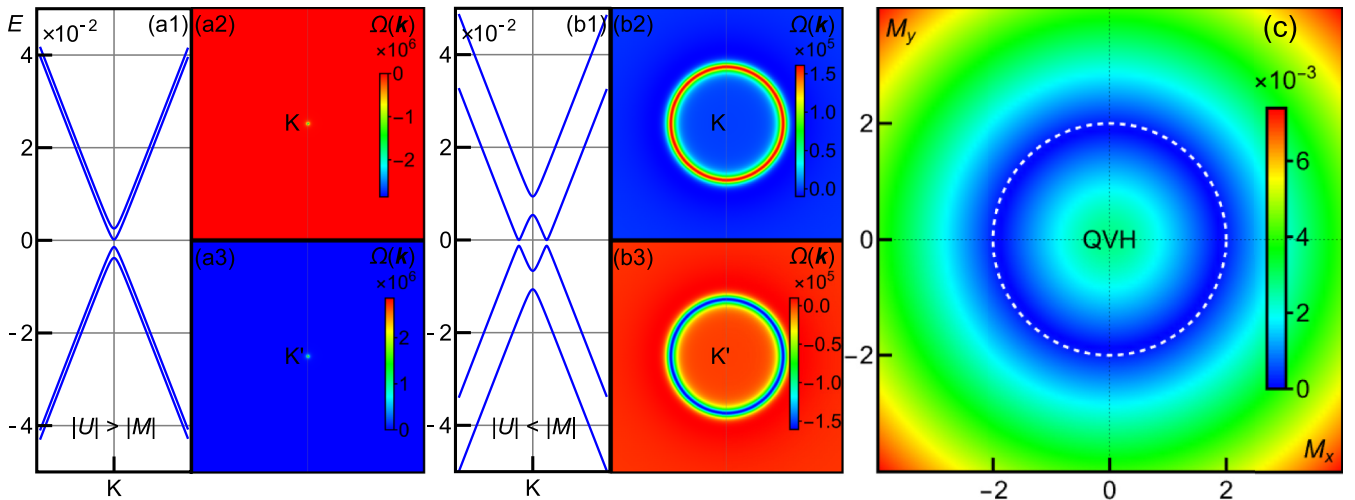


FIG. 1. (a1) Quantum valley Hall, $(C_K, C_{K'}) = (-1, 1)$, with Berry curvature in (a2) and (a3). (b1) An insulating state, neither quantum anomalous Hall nor quantum valley Hall, with Berry curvature in (b2) and (b3). (c) Phase diagram with a circled phase border, with colors encoding the band gap. $\xi_{\text{SOC}} = 0.100$ ($\Delta E_{\text{bulk}} = 0.00164$) and energy in eV.

usual winding number evaluation technique [85] is inapplicable here. Fortunately, we can find, by means of the Wilson loop again, their corresponding Zak phases [45,86] and the result is $\gamma_{\pm} = \pi$.

In summary, the gapless bulk Wannier charge center evolution and the nonvanishing mirror-graded Zak phase jointly confirm consistently that the gapped bulk phase in Fig. 1(b1) is topologically nontrivial, but it is not a Chern insulator either. We then can reasonably expect it to be a second-order topological insulating phase. To find its higher-order embodiment, we next check corresponding systems with spatial dimension reduced.

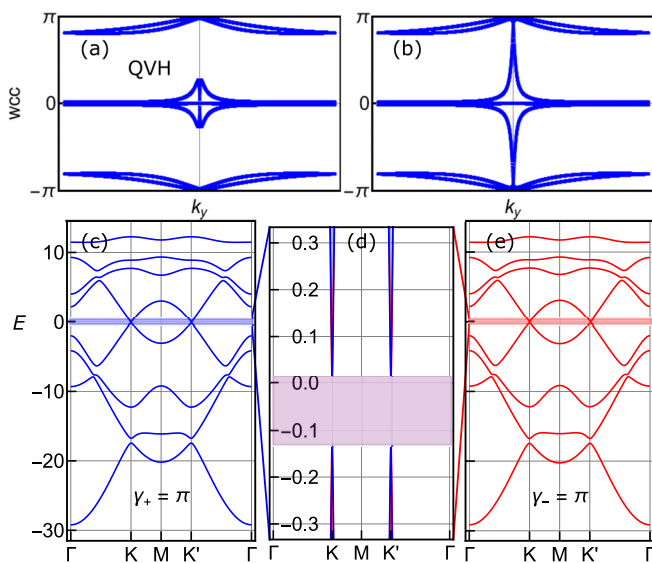


FIG. 2. Characterization of the bulk topology. (a) and (b) Wannier charge center (WCC) evolution for the corresponding phases in Figs. 1(a1) and 1(b1). (c) and (e) Band structures for $H_{\pm}(k_y)$ in Eq. (7), with Zak phases $\gamma_{\pm} = \pi$. (d) Zoom-in for the global gap.

In-gap gapped edge modes with tunability. In the absence of magnetization, the system is in a \mathbb{Z}_2 quantum spin Hall effect, as the Kane-Mele model shows [9,87]. Indeed, our model gives a consistent result that the band structure of a zigzag nanoribbon is gapped out in the bulk and meanwhile the gapless helical edge modes link the valence and conduction bands [Fig. 3(a), gray curves]. However, a major difference emerges because of the absence of particle-hole symmetry that the intersection of the edge modes does not locate within the bulk gap (light-blue region), outside of which as well, consequently, the edge gap is opened up, when the in-plane magnetization takes effect [Fig. 3(b), gray curves]. This situation is harmful to the search for topological corner states located within the edge gap, which contains now also bulk states as well as edge states. By adiabatically introducing an

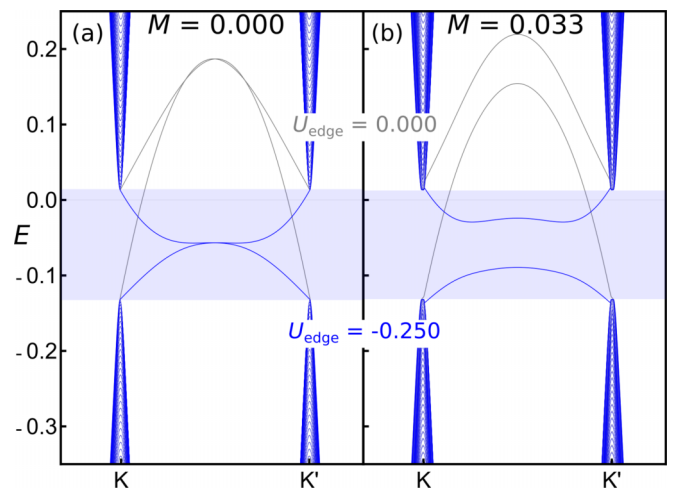


FIG. 3. Band structures of zigzag nanoribbons with tunability of edge modes. (a) Quantum spin Hall effect. (b) Bulk insulating phase from in-plane magnetization. $\xi_{\text{SOC}} = 1.000$ ($\Delta E_{\text{bulk}} = 0.164$) and energy in eV.

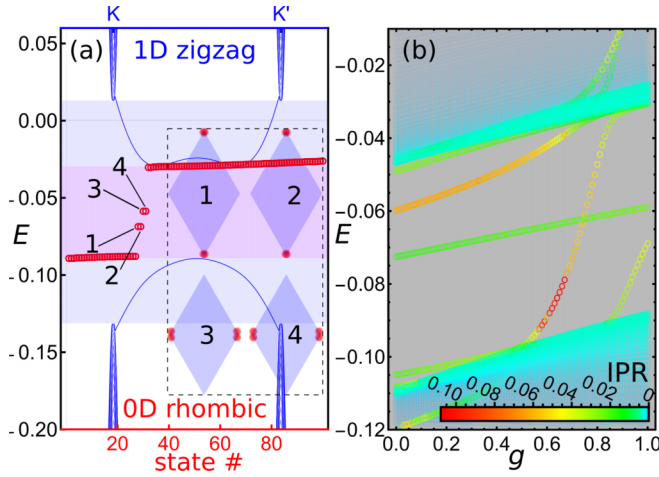


FIG. 4. Topological corner states. (a) The blue band structure is the same as that in Fig. 3(b), red circles show the energy spectrum of a finite zigzag-edged rhombic sheet, and the dashed-framed inset shows the local density of states of corner states. (b) The energy spectrum of the same rhombic finite sheet with $g \in [0, 1]$ in Eq. (2). $\xi_{\text{SOC}} = 1.000$ ($\Delta E_{\text{bulk}} = 0.164$), $M = 0.033$, $U_{\text{edge}} = -0.250$, and energy in eV.

on-site energy difference between the edge and bulk atoms [88,89], the edge modes can be tuned to be inside the bulk gap, regardless of whether or not the edge gap is absent [Figs. 3(a) and 3(b), blue curves]. The bulk band structures exhibit essentially no difference, before and after the introduction of such an on-site energy difference, and as can be seen the blue and the gray bulk almost coincide with each other in Fig. 3. Because such a process is adiabatic, the same topological state maintains.

Anomalous topological corner states. Here, we study the corner states in a rhombic finite sheet edged with zigzag boundaries. In Fig. 4(a), the blue band structure exhibits the dispersion of the corresponding one-dimensional zigzag system, where a clear edge gap (light-red region) within the bulk gap (light-blue region) can be seen. Within this edge gap, four topological corner states appear in the spectrum of a finite rhombic sheet, as the red circles depict, where only a small portion of the states with low energies of interest is presented. Different from the situation reported previously, the four states come in pairs degenerated on nonzero energies. The lower-energy pair (labeled as 1 and 2) takes up the acute diagonal angles, and the higher-energy pair (3 and 4) the obtuse diagonal, as shown respectively in the dashed-framed inset of Fig. 4(a). The four corner states combined together leave no corners of the finite sheet unoccupied.

To reveal the newly emerged acute-angle occupying pair of corner states, we now vary the g factor in Eq. (2) within the unit range $[0, 1]$ to introduce the difference in SOC between the in-plane and the out-of-plane components. As shown in Fig. 4(b), the rightmost case with $g = 1$ is the topological equivalent of that in Fig. 4(a), where the two pairs of corner states have a relatively large inverse participation ratio ($\text{IPR} = \sum_i |\langle \psi | i \rangle|^4$ for a normalized state $|\psi\rangle$ with $\sum_i |\langle \psi | i \rangle|^2 = 1$) [90–94] because of their comparatively high degree of localization and the acute-angle corner state is more localized

than the obtuse-angle one. Furthermore, the spectrum evolves with decreasing g . The edge gap formed between the (green-blue) edge states moves downward as a whole, in which course the (green) obtuse-angle corner states remain in the middle of the gap, indicating the stability of the obtuse-angle corner state in two senses: (i) Its energy position relative to the edge gap, and (ii) its degree of localization, both of which are effectively unaffected. On the other hand, the new acute-angle corner states do not enjoy those two kinds of robustness, because as g changes they change both its relative energy and inverse participation ratio. But in general the acute-angle corner state has a higher degree of localization and a better energy degeneracy. This shows that the acute-angle corner state is more sensitive to the difference between the in-plane and out-of-plane components of spin-orbit coupling.

We further find that both types of corner states are robust against sheet shapes and orbital-dependent magnetization strengths, but the direction of magnetization can control the distribution of the acute-angle corner state. One can see that the two types of corner states are relatively stable because of their topological nature and meanwhile they differ from each other in their own right. More about the effects of sheet-shape and magnetization direction dependencies can be found in the last section of the Supplemental Material [58].

Summary and discussion. We propose the introduction of the bulk-edge on-site energy difference, with experimental feasibility by split-gate technology [95], as a solution to the problem of identifying localized states with higher-order topology in two dimensions when the edge gap position acts as an obstacle. Through a combination of a series of evidence, we show that a second-order topological phase without particle-hole symmetry can be realized in a monolayer graphene system with an in-plane magnetization, but its corner embodiment is not easily found, hidden in the jungle of edge and bulk states. As for the nontrivial bulk topology, we show that the insulating state has a zero Chern number but the behavior of its Wannier charge center is gapless and both mirror-graded subspaces carry a nonvanishing π Zak phase. When mentioning higher-order topology, the “bulk-boundary correspondence” is an unavoidable topic, following which we check the zigzag-edged one- and zero-dimensional systems. In the former we find that, in the region of interest, a clear delineation cannot be achieved between the helical edge crossing and the bulk states. However, we also find that a bulk-edge on-site energy difference can amend it by tuning the edge crossing/gap into the bulk gap window. Then within that gap within a gap, four midgap corner states with nonzero energy degeneracy in pairs can be found unambiguously. Furthermore, we examine the properties of the corner states and find that the obtuse-angle corner state is more stable against a variation of coupling between p_x and p_y orbitals and the direction of in-plane magnetization. Bearing nontrivial topology in nature, both types are robust with respect to the shapes of the finite sheets. These results not only suggest an accessible way to “find” corner states, but also provide a sample which a future full-fledged higher-order topological version of bulk-boundary correspondence should take into account. Our findings are not limited to electronic systems or two

dimensions, and should also be of importance to higher-order topology in phononic and photonic crystals, due to similar governing laws.

Acknowledgments. This work was financially supported by the National Natural Science Foundation of China (No. 11974327, No. 12074241, and No. 11929401), Fun-

damental Research Funds for the Central Universities (WK3510000010, WK2030020032), Anhui Initiative in Quantum Information Technologies. We also thank the supercomputing service of AM-HPC and the Supercomputing Center of University of Science and Technology of China for providing the high-performance computing resources.

- [1] M. Nakahara, *Geometry, Topology and Physics*, 2nd ed. (CRC Press/Taylor & Francis, Boca Raton, FL, 2003).
- [2] M. Fruchart and D. Carpentier, *C. R. Phys.* **14**, 779 (2013).
- [3] C. Zhao, [arXiv:1309.2056](https://arxiv.org/abs/1309.2056).
- [4] R. M. Kaufmann and D. Li, *Rev. Math. Phys.* **28**, 1630003 (2016).
- [5] J. Cayssol and J. N. Fuchs, *J. Phys. Mater.* **4**, 034007 (2021).
- [6] C.-X. Liu, S.-C. Zhang, and X.-L. Qi, *Annu. Rev. Condens. Matter Phys.* **7**, 301 (2016).
- [7] C.-Z. Chang, J. Zhang, X. Feng, J. Shen, Z. Zhang, M. Guo, K. Li, Y. Ou, P. Wei, L.-L. Wang, Z.-Q. Ji, Y. Feng, S. Ji, X. Chen, J. Jia, X. Dai, Z. Fang, S.-C. Zhang, K. He, Y. Wang *et al.*, *Science* **340**, 167 (2013).
- [8] Z. Qiao, S. A. Yang, W. Feng, W.-K. Tse, J. Ding, Y. Yao, J. Wang, and Q. Niu, *Phys. Rev. B* **82**, 161414(R) (2010).
- [9] C. L. Kane and E. J. Mele, *Phys. Rev. Lett.* **95**, 226801 (2005).
- [10] B. A. Bernevig and S.-C. Zhang, *Phys. Rev. Lett.* **96**, 106802 (2006).
- [11] M. König, S. Wiedmann, C. Brüne, A. Roth, H. Buhmann, L. W. Molenkamp, X.-L. Qi, and S.-C. Zhang, *Science* **318**, 766 (2007).
- [12] D. J. Thouless, M. Kohmoto, M. P. Nightingale, and M. den Nijs, *Phys. Rev. Lett.* **49**, 405 (1982).
- [13] B. Simon, *Phys. Rev. Lett.* **51**, 2167 (1983).
- [14] C. L. Kane and E. J. Mele, *Phys. Rev. Lett.* **95**, 146802 (2005).
- [15] L. Fu and C. L. Kane, *Phys. Rev. B* **76**, 045302 (2007).
- [16] J. E. Moore and L. Balents, *Phys. Rev. B* **75**, 121306(R) (2007).
- [17] X.-L. Qi, Y.-S. Wu, and S.-C. Zhang, *Phys. Rev. B* **74**, 045125 (2006).
- [18] J. C. Y. Teo and C. L. Kane, *Phys. Rev. B* **82**, 115120 (2010).
- [19] T. Fukui, K. Shiozaki, T. Fujiwara, and S. Fujimoto, *J. Phys. Soc. Jpn.* **81**, 114602 (2012).
- [20] G. M. Graf and M. Porta, *Commun. Math. Phys.* **324**, 851 (2013).
- [21] J.-W. Rhim, J. H. Bardarson, and R.-J. Slager, *Phys. Rev. B* **97**, 115143 (2018).
- [22] C. Max, Bulk-boundary correspondence of disordered topological insulators and superconductors, Ph.D. thesis, Universität zu Köln, 2019.
- [23] A. Alase, Boundary physics and bulk-boundary correspondence in topological phases of matter, Ph.D. thesis, Dartmouth College, 2019.
- [24] M. G. Silveirinha, *Phys. Rev. X* **9**, 011037 (2019).
- [25] S. Yao and Z. Wang, *Phys. Rev. Lett.* **121**, 086803 (2018).
- [26] Y. Xiong, *J. Phys. Commun.* **2**, 035043 (2018).
- [27] F. K. Kunst, E. Edvardsson, J. C. Budich, and E. J. Bergholtz, *Phys. Rev. Lett.* **121**, 026808 (2018).
- [28] K.-I. Imura and Y. Takane, *Phys. Rev. B* **100**, 165430 (2019).
- [29] P. Gao, M. Willatzen, and J. Christensen, *Phys. Rev. Lett.* **125**, 206402 (2020).
- [30] L. Xiao, T. Deng, K. Wang, G. Zhu, Z. Wang, W. Yi, and P. Xue, *Nat. Phys.* **16**, 761 (2020).
- [31] M. Kim, Z. Jacob, and J. Rho, *Light: Sci. Appl.* **9**, 130 (2020).
- [32] E. Lee, R. Kim, J. Ahn, and B.-J. Yang, *npj Quantum Mater.* **5**, 1 (2020).
- [33] M. J. Park, Y. Kim, G. Y. Cho, and S. B. Lee, *Phys. Rev. Lett.* **123**, 216803 (2019).
- [34] Y. Otaki and T. Fukui, *Phys. Rev. B* **100**, 245108 (2019).
- [35] F. Schindler, A. M. Cook, M. G. Vergniory, Z. Wang, S. S. P. Parkin, B. A. Bernevig, and T. Neupert, *Sci. Adv.* **4**, eaat0346 (2018).
- [36] F. Schindler, *J. Appl. Phys.* **128**, 221102 (2020).
- [37] W. A. Benalcazar, B. A. Bernevig, and T. L. Hughes, *Science* **357**, 61 (2017).
- [38] S. Qian, C.-C. Liu, and Y. Yao, *Phys. Rev. B* **104**, 245427 (2021).
- [39] Y. Ren, Z. Qiao, and Q. Niu, *Phys. Rev. Lett.* **124**, 166804 (2020).
- [40] Y. Tanaka, R. Takahashi, and S. Murakami, *Phys. Rev. B* **101**, 115120 (2020).
- [41] K. Plekhanov, F. Ronetti, D. Loss, and J. Klinovaja, *Phys. Rev. Res.* **2**, 013083 (2020).
- [42] C. Yue, Y. Xu, Z. Song, H. Weng, Y.-M. Lu, C. Fang, and X. Dai, *Nat. Phys.* **15**, 577 (2019).
- [43] G. Pelegrí, A. M. Marques, V. Ahufinger, J. Mompart, and R. G. Dias, *Phys. Rev. B* **100**, 205109 (2019).
- [44] X.-W. Luo and C. Zhang, *Phys. Rev. Lett.* **123**, 073601 (2019).
- [45] X.-L. Sheng, C. Chen, H. Liu, Z. Chen, Z. M. Yu, Y. X. Zhao, and S. A. Yang, *Phys. Rev. Lett.* **123**, 256402 (2019).
- [46] C. Chen, Z. Song, J.-Z. Zhao, Z. Chen, Z.-M. Yu, X.-L. Sheng, and S. A. Yang, *Phys. Rev. Lett.* **125**, 056402 (2020).
- [47] F. D. M. Haldane, *Phys. Rev. Lett.* **61**, 2015 (1988).
- [48] Z. Qiao, W.-K. Tse, H. Jiang, Y. Yao, and Q. Niu, *Phys. Rev. Lett.* **107**, 256801 (2011).
- [49] W.-K. Tse, Z. Qiao, Y. Yao, A. H. MacDonald, and Q. Niu, *Phys. Rev. B* **83**, 155447 (2011).
- [50] Z. Qiao, H. Jiang, X. Li, Y. Yao, and Q. Niu, *Phys. Rev. B* **85**, 115439 (2012).
- [51] Z. Qiao, X. Li, W.-K. Tse, H. Jiang, Y. Yao, and Q. Niu, *Phys. Rev. B* **87**, 125405 (2013).
- [52] X. Deng, S. Qi, Y. Han, K. Zhang, X. Xu, and Z. Qiao, *Phys. Rev. B* **95**, 121410(R) (2017).
- [53] J. Zeng, Y. Ren, K. Zhang, and Z. Qiao, *Phys. Rev. B* **95**, 045424 (2017).
- [54] F. Liu and K. Wakabayashi, *Phys. Rev. Res.* **3**, 023121 (2021).
- [55] M. Pan, D. Li, J. Fan, and H. Huang, *npj Comput. Mater.* **8**, 1 (2022).

- [56] Z. Qiao, W. Ren, H. Chen, L. Bellaïche, Z. Zhang, A. H. MacDonald, and Q. Niu, *Phys. Rev. Lett.* **112**, 116404 (2014).
- [57] C. Chen, J. Zeng, Y. Ren, L. Fang, Y. Wu, P. Zhang, T. Hu, J. Wang, Z. Qiao, and W. Ren, *Appl. Phys. Lett.* **120**, 084002 (2022).
- [58] See Supplemental Material at <http://link.aps.org/supplemental/10.1103/PhysRevB.106.L201407> for technical details as well as extra properties of corner states, which includes Refs. [96–102].
- [59] B. Xie, G. Su, H.-F. Wang, F. Liu, L. Hu, S.-Y. Yu, P. Zhan, M.-H. Lu, Z. Wang, and Y.-F. Chen, *Nat. Commun.* **11**, 3768 (2020).
- [60] R. Tao and P. Sheng, *J. Acoust. Soc. Am.* **77**, 1651 (1985).
- [61] M. S. Kushwaha, P. Halevi, L. Dobrzynski, and B. Djafari-Rouhani, *Phys. Rev. Lett.* **71**, 2022 (1993).
- [62] M. Born and K. Huang, *Dynamical Theory of Crystal Lattices* (Oxford University Press, Oxford, U.K., 1962).
- [63] Z. Li, *Solid State Theory*, 2nd ed. (Higher Education Press, Beijing, 2009).
- [64] P. A. Deymier, *Acoustic Metamaterials and Phononic Crystals* (Springer, Berlin, 2013).
- [65] A. Khelif and A. Adibi, *Phononic Crystals: Fundamentals and Applications* (Springer, Berlin, 2016).
- [66] J. D. Joannopoulos, S. G. Johnson, J. N. Winn, and R. D. Meade, *Photonic Crystals: Molding the Flow of Light*, 2nd ed. (Princeton University Press, Princeton, NJ, 2008).
- [67] M. Skorobogatiy and J. Yang, *Fundamentals of Photonic Crystal Guiding* (Cambridge University Press, Cambridge, U.K., 2009).
- [68] P. Wang, L. Lu, and K. Bertoldi, *Phys. Rev. Lett.* **115**, 104302 (2015).
- [69] Z. Yang, F. Gao, X. Shi, X. Lin, Z. Gao, Y. Chong, and B. Zhang, *Phys. Rev. Lett.* **114**, 114301 (2015).
- [70] L. Lu, C. Fang, L. Fu, S. G. Johnson, J. D. Joannopoulos, and M. Soljai, *Nat. Phys.* **12**, 337 (2016).
- [71] A. Slobozhanyuk, S. H. Mousavi, X. Ni, D. Smirnova, Y. S. Kivshar, and A. B. Khanikaev, *Nat. Photonics* **11**, 130 (2017).
- [72] J. C. Slater and G. F. Koster, *Phys. Rev.* **94**, 1498 (1954).
- [73] R. Saito, G. Dresselhaus, and M. S. Dresselhaus, *Physical Properties of Carbon Nanotubes* (Imperial College Press, London, 1998).
- [74] W. A. Harrison, *Elementary Electronic Structure* (World Scientific, Singapore, 1999).
- [75] P. Zhong, Y. Ren, Y. Han, L. Zhang, and Z. Qiao, *Phys. Rev. B* **96**, 241103(R) (2017).
- [76] C.-C. Liu, H. Jiang, and Y. Yao, *Phys. Rev. B* **84**, 195430 (2011).
- [77] S. Konschuh, M. Gmitra, and J. Fabian, *Phys. Rev. B* **82**, 245412 (2010).
- [78] H. Min, J. E. Hill, N. A. Sinitsyn, B. R. Sahu, L. Kleinman, and A. H. MacDonald, *Phys. Rev. B* **74**, 165310 (2006).
- [79] M. V. Berry, *Proc. R. Soc. Lond. A* **392**, 45 (1984).
- [80] H. Jiang, Z. Qiao, H. Liu, and Q. Niu, *Phys. Rev. B* **85**, 045445 (2012).
- [81] R. Yu, X. L. Qi, A. Bernevig, Z. Fang, and X. Dai, *Phys. Rev. B* **84**, 075119 (2011).
- [82] H.-X. Wang, G.-Y. Guo, and J.-H. Jiang, *New J. Phys.* **21**, 093029 (2019).
- [83] M. S. Dresselhaus, G. Dresselhaus, and A. Jorio, *Group Theory: Application to the Physics of Condensed Matter* (Springer, Berlin, 2008).
- [84] X. Li, *Group Theory and Its Application to Condensed Matter Physics* (Peking University Press, Beijing, 2019).
- [85] J. Song and E. Prodan, *Phys. Rev. B* **89**, 224203 (2014).
- [86] J. Zak, *Phys. Rev. Lett.* **62**, 2747 (1989).
- [87] L. Brey, P. Seneor, and A. Tejeda, *Graphene Nanoribbons* (IOP Publishing, Bristol, U.K., 2020).
- [88] P. A. Pantaleón and Y. Xian, *Phys. B: Condens. Matter* **530**, 191 (2018).
- [89] P. A. Pantaleón and Y. Xian, *J. Phys. Soc. Jpn.* **87**, 064005 (2018).
- [90] J. T. Edwards and D. J. Thouless, *J. Phys. C: Solid State Phys.* **5**, 807 (1972).
- [91] N. C. Murphy, R. Wortis, and W. A. Atkinson, *Phys. Rev. B* **83**, 184206 (2011).
- [92] M. Calixto and E. Romera, *J. Stat. Mech.* **2015**, P06029 (2015).
- [93] G. Misguich, V. Pasquier, and J.-M. Luck, *Phys. Rev. B* **94**, 155110 (2016).
- [94] E. Tsukerman, *Phys. Rev. B* **95**, 115121 (2017).
- [95] J. Li, K. Wang, K. J. McFaul, Z. Zern, Y. Ren, K. Watanabe, T. Taniguchi, Z. Qiao, and J. Zhu, *Nat. Nanotechnol.* **11**, 1060 (2016).
- [96] P. E. Blöchl, *Phys. Rev. B* **50**, 17953 (1994).
- [97] G. Kresse and J. Furthmüller, *Phys. Rev. B* **54**, 11169 (1996).
- [98] J. P. Perdew, J. A. Chevary, S. H. Vosko, K. A. Jackson, M. R. Pederson, D. J. Singh, and C. Fiolhais, *Phys. Rev. B* **46**, 6671 (1992).
- [99] J. P. Perdew, K. Burke, and M. Ernzerhof, *Phys. Rev. Lett.* **77**, 3865 (1996).
- [100] S. Grimme, *J. Comput. Chem.* **27**, 1787 (2006).
- [101] A. A. Mostofi, J. R. Yates, Y. S. Lee, I. Souza, D. Vanderbilt, and N. Marzari, *Comput. Phys. Commun.* **178**, 685 (2008).
- [102] X.-P. Li, D.-S. Ma, C.-C. Liu, Z.-M. Yu, and Y. Yao, *Phys. Rev. B* **105**, 165135 (2022).